6-2012

Long-term correction of very long-chain acyl-coA dehydrogenase deficiency in mice using AAV9 gene therapy

Allison M. Keeler
University of Massachusetts Medical School

Thomas J. Conlon
University of Florida

Glenn Walter
University of Florida

See next page for additional authors

Long-term correction of very long-chain acyl-coA dehydrogenase deficiency in mice using AAV9 gene therapy

Authors
Allison M. Keeler, Thomas J. Conlon, Glenn Walter, Huadong Zeng, Scott A. Shaffer, Fu Dungtao, Kirsten E. Erger, Travis L. Cossette, Qiushi Tang, Christian Mueller, and Terence R. Flotte

MTOpen

original article

Long-term Correction of Very Long-chain Acyl-CoA Dehydrogenase Deficiency in Mice Using AAV9 Gene Therapy

Allison M Keeler[1], Thomas Conlon[2], Glenn Walter[3,4], Huadong Zeng[4], Scott A Shaffer[5], Fu Dungtao[6], Kirsten Erger[2], Travis Cossette[2], Qiushi Tang[1], Christian Mueller[1] and Terence R Flotte[1]

[1]Gene Therapy Center, Department of Pediatrics, University of Massachusetts Medical School, Worcester, Massachusetts, USA; [2]Powell Gene Therapy Center, Department of Pediatrics, University of Florida, Gainesville, Florida, USA; [3]Department of Physiology and Functional Genomics, University of Florida, Gainesville, Florida, USA; [4]National High Magnetic Field Laboratory, University of Florida, Gainesville, Florida, USA; [5]Proteomics and Mass Spectrometry Facility, Department of Biochemistry and Molecular Pharmacology, University of Massachusetts Medical School, Worcester, Massachusetts, USA; [6]Department of Pathology, University of Florida, Gainesville, Florida, USA

Very long-chain acyl-coA dehydrogenase (VLCAD) is the rate-limiting step in mitochondrial fatty acid oxidation. VLCAD-deficient mice and patients clinical symptoms stem from not only an energy deficiency but also long-chain metabolite accumulations. VLCAD-deficient mice were treated systemically with 1×10^{12} vector genomes of recombinant adeno-associated virus 9 (rAAV9)-VLCAD. Biochemical correction was observed in vector-treated mice beginning 2 weeks postinjection, as characterized by a significant drop in long-chain fatty acyl accumulates in whole blood after an overnight fast. Changes persisted through the termination point around 20 weeks postinjection. Magnetic resonance spectroscopy (MRS) and tandem mass spectrometry (MS/MS) revealed normalization of intramuscular lipids in treated animals. Correction was not observed in liver tissue extracts, but cardiac muscle extracts showed significant reduction of long-chain metabolites. Disease-specific phenotypes were characterized, including thermoregulation and maintenance of euglycemia after a fasting cold challenge. Internal body temperatures of untreated VLCAD$^{-/-}$ mice dropped below 20 °C and the mice became lethargic, requiring euthanasia. In contrast, all rAAV9-treated VLCAD$^{-/-}$ mice and the wild-type controls maintained body temperatures. rAAV9-treated VLCAD$^{-/-}$ mice maintained euglycemia, whereas untreated VLCAD$^{-/-}$ mice suffered hypoglycemia following a fasting cold challenge. These promising results suggest rAAV9 gene therapy as a potential treatment for VLCAD deficiency in humans.

Received 15 December 2011; accepted 6 February 2012; advance online publication 6 March 2012. doi:10.1038/mt.2012.39

INTRODUCTION

Very long-chain acyl-coA dehydrogenase (VLCAD) deficiency is the most common disorder of long-chain fatty acid metabolism, with a regional incidence of 1 in 30,000 births, and second in frequency only to medium-chain acyl-coA dehydrogenase deficiency among disorders of fatty acid oxidation.[1,2] Characterized by the most severe phenotype within the acyl-coA dehydrogenase deficiency family, patients generally present with one of three distinct clinical phenotypes. Of these three phenotypes the early onset presentation during infancy is the most severe, presenting with cardiomyopathy and hepatopathy and are often fatal.[3] A less severe hepatic phenotype presenting with recurrent hypoketotic hypoglycemia, also occurs in infancy to early childhood. The third phenotype is a mild, myopathic form presenting in adolescence or adulthood with muscle weakness, myalgia and myoglobinuria.[4,5]

VLCAD is responsible for catabolism of long-chain fatty acids, with highest specificity for carbon lengths C14–C18, as part of the mitochondrial β-oxidation spiral. It is the rate-limiting enzyme in the process, causing an energy deficiency as well as accumulations of long-chain fatty acids. β-Oxidation is an important source of energy for liver and muscle, especially cardiac muscle. The disease is associated with a lack of energy caused by the inability to breakdown long-chain fatty acids but the accumulates of these long-chain fatty acids can also be detrimental.[6,7] The amassments of these metabolites are exploited for diagnostic purposes as part of the newborn screening by analyzing for acyl carnitine metabolite accumulations in the blood by tandem mass spectrometry (MS/MS). Although newborn screening has reduced mortality, the current treatment is limited to fasting avoidance, and supplementation of medium-chain triglycerides, which remains controversial since supplementation of medium-chain triglycerides in excess of the immediate caloric demand will induce the production of longer chain fatty acids for storage as triglycerides.[8] These in turn will add to the total load of longer chain fatty acids, which cannot be subsequently metabolized when caloric restriction occurs. Therefore, VLCAD deficiency is a candidate for gene therapy because of its limited treatment options as well as its potentially fatal phenotype.

We have previously shown biochemical correction of short-chain acyl-coA dehydrogenase deficiency by targeting muscle with recombinant adeno-associated virus 1 (rAAV1) and rAAV2,

Correspondence: *Terence R Flotte, University of Massachusetts Medical School, University Campus-S1-340, 55 Lake Avenue North, Worcester, Massachusetts, USA. E-mail: terry.flotte@umassmed.edu*

and liver with rAAV8 as well as long-chain acyl-coA dehydrogenase deficiency by targeting the muscle with rAAV1.[9–11] New AAV serotypes, such as AAV9, have improved expression and wider transduction profiles.[12,13] Merritt and colleagues[14] showed limited biochemical correction of VLCAD deficiency using systemic injections with AAV8. Here, we present the first evidence of a genetic therapy that systemically targets major tissues involved in β-oxidation, has long-term expression and corrects several disease-specific phenotypes in a VLCAD-deficient mouse model.

RESULTS

Differential expression, transduction, and tissue distribution of rAAV9-VLCAD

To assess the therapeutic benefit of rAAV9-VLCAD complementary DNA delivery, 6–8-week-old VLCAD$^{-/-}$ or VLCAD$^{+/+}$ littermate controls were injected into the tail vein with either rAAV9-CBA-VLCAD (1×10^{12} vector genomes) as a therapeutic agent or rAAV9-CBA green fluorescent protein or phosphate-buffered saline (PBS) as controls. Quantitative real-time PCR was performed on genomic DNA (gDNA) isolated from multiple tissues at 22–26 weeks postinjection to determine tissue distribution of vector genomes (**Figure 1a**). All tissues were negative for vector genomes in PBS VLCAD$^{-/-}$ or PBS VLCAD$^{+/+}$ controls. In mice injected with rAAV9-VLCAD, the highest vector genome concentration in tissues associated with fatty acid oxidation was observed in the liver, followed by heart, skeletal muscle, and brown fat. Expression is shown by human VLCAD antibody staining of the liver, heart, tibialis anterior muscle, and brown fat (**Figure 1b–i**). Also vector genomes were found present in tissues not associated with fatty acid oxidation including gonads, lung, spleen, and lymph nodes (**Figure 1a**). Although transduction of the liver had the highest transduction among the tissues, liver expression was not widespread, with numerous cells expressing VLCAD at high levels while others did not express VLCAD (**Figure 1c**). Expression of VLCAD in the heart and tibialis anterior was widespread (**Figure 1e,g**). Interestingly, transduction and expression were seen in the brown fat (**Figure 1h,i**). Liver and muscle were also stained with hematoxylin and eosin and scored by a blinded pathologist for inflammation (**Supplementary Figure S1**). Some inflammation was seen across all groups and no significant difference was seen in inflammation between PBS control and AAV9-VLCAD treated VLCAD$^{-/-}$ in the liver. No inflammation was seen in any group within the muscle. Taken together, these results indicate that rAAV9-VLCAD vectors were able to sufficiently transduce and express for over 6 months in vital organs, which rely on fatty acid oxidation.

Correction of acyl carnitine accumulates in the blood

Because VLCAD-deficient patients have a greater magnitude of accumulation of long-chain acyl carnitines in the blood, it was essential to demonstrate biochemical correction of whole blood by measuring acyl carnitine accumulates by electrospray MS/MS. Before treatment, and on days 14, 42, and 140 postinjection, mice were subjected to a 24-hour fast followed by whole blood collection. Metabolic stress such as fasting was required to observe optimal response. Large accumulations of long-chain metabolites were found in VLCAD$^{-/-}$ PBS controls and reductions of the levels of C14, C16:1, C16, C18:2, C18:1, and C18 were seen 14 days postinjection in rAAV9-treated VLCAD$^{-/-}$ animals when compared to VLCAD$^{-/-}$ PBS controls (**Figure 2a**). There were no significant differences between controls, AAV9-green fluorescent protein or PBS, so PBS was used as a control for subsequent experiments (**Supplementary Figure S2a–c**). It was noted that reductions in blood acyl carnitines were observed across all groups between the first and second 24-hour fasting time points, regardless of treatment, age, or if mice remained uninjected (**Figure 3a** and **Supplementary Figure S3a–f**), a phenomena that is also observed in our medium-chain acyl-coA dehydrogenase deficiency mice. Significant reductions in levels of C16, C18:1, C18 (**Figure 2b–d**, $P < 0.0006$; **Supplementary Figure S2a–c**) in whole

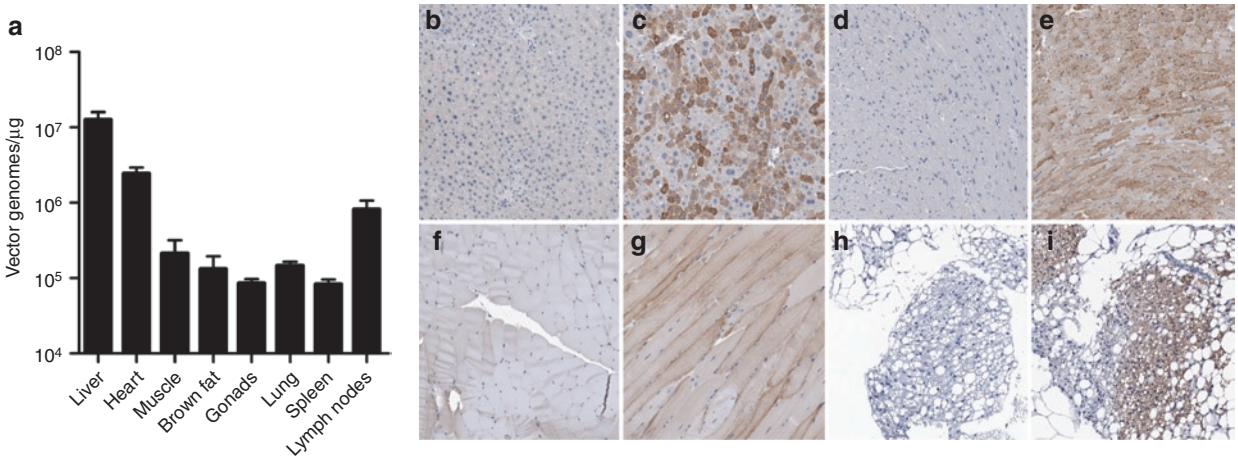

Figure 1 Transduction and expression of rAAV9-VLCAD. (**a**) Quantitative-PCR for vector genomes. Means of three separate assays ± SEM are shown for each organ. $n = 7$ VLCAD$^{-/-}$ phosphate-buffered saline (PBS) control, 6 VLCAD$^{-/-}$ rAAV9-VLCAD treated and VLCAD$^{+/+}$ PBS control. Only VLCAD$^{-/-}$ rAAV9 treated are shown, as PBS controls were all negative. Error bars are SEM. (**b–i**) Representative images of very long-chain acyl-coA dehydrogenase (VLCAD) antibody staining in VLCAD$^{-/-}$ mice, 21–26 weeks postinjection, 5× magnification. (**b**) Liver PBS control. (**c**) Liver, rAAV9-VLCAD treated. (**d**) Heart, PBS control. (**e**) Heart, rAAV9-VLCAD treated. (**f**) Tibialis anterior (TA) muscle, PBS control. (**g**) TA, rAAV9-VLCAD treated. (**h**) Brown fat, PBS control. (**i**) Brown fat, rAAV9-VLCAD treated.

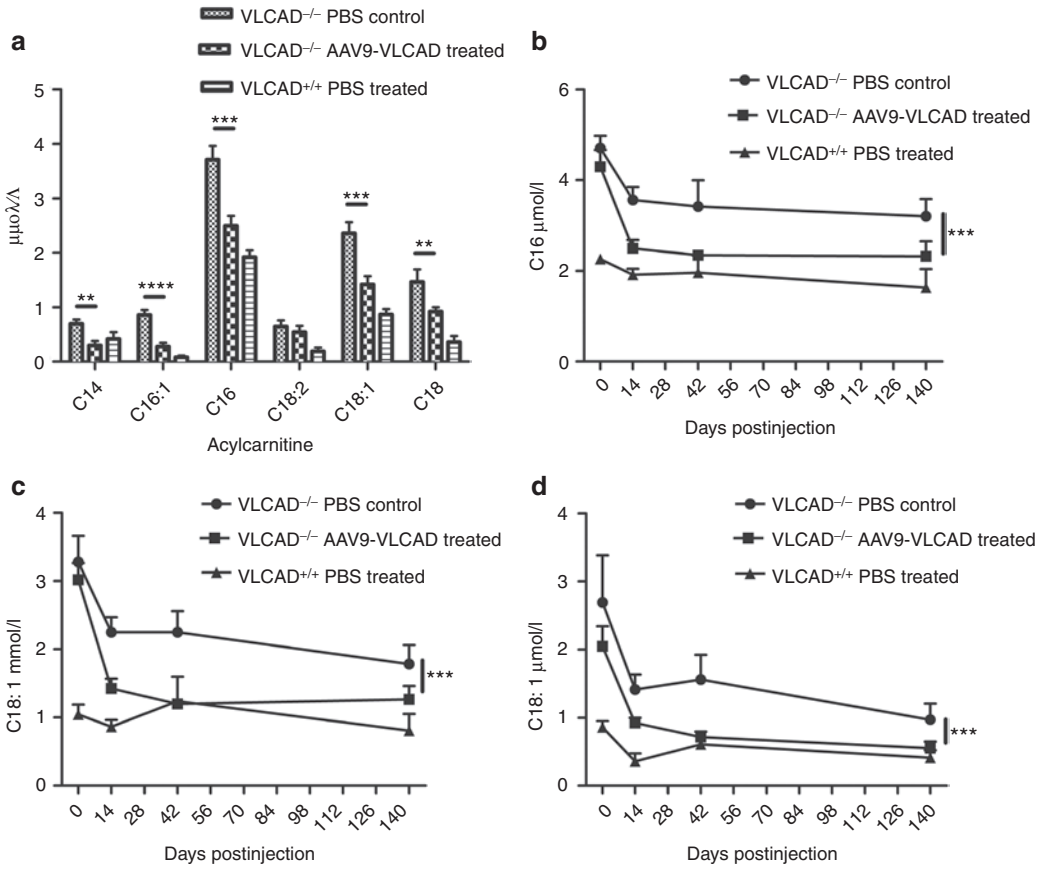

Figure 2 Reduction of acyl carnitines in rAAV9-very long-chain acyl-coA dehydrogenase (VLCAD)-treated mice. All animals were fasted 24 hours before bleeding. *$P < 0.05$, **$P < 0.01$, ***$P < 0.001$, ****$P < 0.0001$. (**a**) Quantities of acyl carnitine species as assessed by mass spectrometry of whole blood day 14 postinjection. $n = 7$ untreated VLCAD$^{-/-}$ controls, $n = 6$ rAAV9-treated VLCAD$^{-/-}$ mice; and $n = 6$ in wild-type controls. Error bars are SEM. P values are as follows: C14 $P = 0.002$, C16:1 $P \leq 0.0001$ C16 $P = 0.0008$ C18:2 $P = 0.005$, C18:1 $P = 0.005$, C18 $P = 0.04$. (**b–d**) Untreated VLCAD$^{-/-}$ controls day 0 and 14 $n = 11$; day 6 $n = 3$; D140 $n = 7$. rAAV9-treated VLCAD$^{-/-}$ mice day 0 and 14 $n = 11$; day 6 $n = 5$; D140 $n = 6$. Wild-type control mice day 0, 14 $n = 11$; day 6 $n = 5$; D140 $n = 6$. (**b**) Mass spectrometric quantification of C16 in the whole blood over time. Error bars are SEM. A two-way analysis of variance (ANOVA) was performed on data from day 14–day 140 with $P = 0.0006$. (**c**) Mass spectrometric quantification of C18:1 over time. Error bars are SEM. A two-way ANOVA was performed on data from day 14–day 140 with $P = 0.0003$. (**d**) Mass spectrometric quantification of C18 over time. Error bars are SEM. A two-way ANOVA was performed on data from day 14–day 140 with $P = 0.0014$.

blood persisted for over 140 days postinjection of rAAV9-VLCAD when compared to the PBS controls. These reductions, which were observed out to 140 days postinjection, infer biochemical correction of the whole blood.

Tissue correction *in vivo* and *ex vivo*

Biochemical correction within the liver tissue itself was assessed by an *in vivo* and *ex vivo* approach. Using single voxel proton magnetic resonance spectroscopy (^{1}H-MRS), lipid accumulations in the liver were measured in live animals 17 weeks postinjection. **Figure 3a** shows representative liver spectra from VLCAD$^{-/-}$ PBS control, VLCAD$^{-/-}$ AAV9-treated and VLCAD$^{+/+}$ PBS control mice. A measure of total lipid, the ratio of the area under the lipid peak divided by the area under the water peak, as an internal control is shown in **Figure 3b**. No significant differences were seen in accumulations measured by MRS between the VLCAD$^{-/-}$ and VLCAD$^{+/+}$ or rAAV9-treated groups. *Ex vivo* acyl carnitine accumulations were measured by MS/MS of the liver tissue. Significant differences in reduction of C16, C18:2, C18:1, and C18 were observed between the VLCAD$^{-/-}$ PBS control and VLCAD$^{+/+}$ mice (**Figure 3c**). Unexpectedly, reductions were not seen in the liver of the VLCAD$^{-/-}$ rAAV9-treated animals, despite the significant reductions seen in whole blood.

Analogously, we assessed biochemical correction in the muscle tissue employing the same *in vivo*/*ex vivo* approach. **Figure 4a** is an magnetic resonance image of a representative muscle, with the box indicating the location within the muscle where the ^{1}H-MRS spectrum was taken. Representative spectra from VLCAD$^{-/-}$ PBS control, VLCAD$^{-/-}$ rAAV9-treated and VLCAD$^{+/+}$ PBS control mice are shown in **Figure 4b**. The ratio of the area under the lipid peak was divided by the area under the taurine, trimethyl ammonium, and creatine total peak, as the internal control for muscle. Comparison of VLCAD$^{-/-}$ PBS control, VLCAD$^{-/-}$ rAAV9-treated, and VLCAD$^{+/+}$ PBS control mice, lipid peak ratios are shown in **Figure 4c**. The VLCAD$^{-/-}$ PBS control mice had accumulation of lipids within the muscle whereas the VLCAD$^{-/-}$ rAAV9 treated exhibited reduced lipid content similar to wild-type mice. Acyl carnitine accumulations were observed from *ex vivo* tissue by MS/MS for both the extensor digitorum longus, primarily composed of fast twitch muscle, and the soleus, primarily composed of

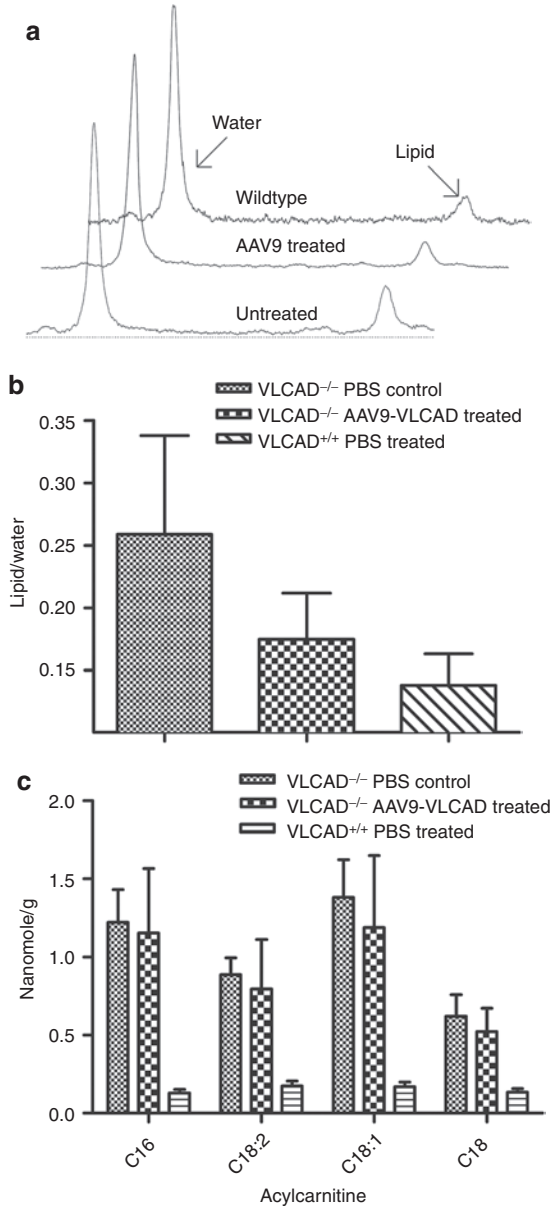

Figure 3 Biochemical analysis of acyl carnitines in the liver *in vivo* and *ex vivo*. (**a**) Representative spectra from magnetic resonance spectrometry of liver *in vivo*. 17–18 weeks postinjection. (**b**) Quantification of the ratio of the area of the lipid peak/area of the water peak. Error bars are SEM. $n = 3$. (**c**) Mass spectrometric analysis of liver tissue *ex vivo*, 21–25 weeks postinjection; $n = 7$ untreated VLCAD$^{-/-}$ controls, $n = 6$ rAAV9-treated VLCAD$^{-/-}$ and wild-type controls. Error bars are SEM. Samples were analyzed in triplicate. VLCAD, very long-chain acyl-coA dehydrogenase.

slow twitch fibers. Reductions of long-chain accumulations were observed in both the extensor digitorum longus (**Figure 4d**) and soleus (**Figure 4e**) in the rAAV9-treated animals. Furthermore, expression of VLCAD in the skeletal muscle reduced accumulations of acyl carnitines within the tissue.

Cardiomyopathy can be a presenting symptom in patients with VLCAD deficiency.[15,16] Since expression was widespread in the heart (**Figure 1e**), a question remained if biochemical correction of the cardiac tissue had occurred. Cardiac tissue was analyzed by MS/MS of acyl carnitines extracted from *ex vivo* tissue. Acyl carnitines in cardiac muscle were at or below wild-type levels in rAAV9-treated mice whereas VLCAD$^{-/-}$ PBS controls had large accumulations (**Figure 5**). Expression of VLCAD in cardiac muscle, facilitated by rAAV9, was able to correct VLCAD$^{-/-}$ animals to wild-type levels of acyl carnitines in the cardiac tissue instead of large accumulations seen in VLCAD$^{-/-}$ animals.

Disease-specific phenotypic correction of VLCAD deficiency

Cold can induce metabolic derangement in VLCAD deficiency patients, as production of heat requires fatty acid oxidation especially after dietary fat stores have been used up.[17] VLCAD-deficient mice are also unable to maintain body temperatures during a cold challenge, and it has been shown to be fatal especially when combined with fasting.[18] To assay for disease-specific phenotypic correction, a cold fast challenge was utilized, in which the mice are fasted for 18 hours followed by a cold challenge in a 4 °C room. During the challenge, a humane sacrifice was performed for animals with a body temperature below 20 °C as determined by Institutional Animal Care and Use Committee (IACUC). In **Figure 6a**, the VLCAD$^{-/-}$ AAV9-treated and wild-type animals were able to maintain average body temperatures of 26.15 and 26.4 °C, respectively for 150 minutes. However, PBS control VLCAD$^{-/-}$ animals were unable to maintain body temperatures above 20 °C, with two animals being euthanized at 110 minutes and the remaining two animals at 130 minutes. To summarize, by 150 minutes into the cold challenge all of the PBS control VLCAD$^{-/-}$ animals had internal temperatures that dropped below the humane sacrifice point, whereas all the VLCAD$^{-/-}$ AAV9-treated, and wild-type animals survived (**Figure 6b**). Lethargy and hypotonia are often a presenting symptom when VLCAD-deficient patients are undergoing a period of metabolic crisis.[7] PBS control VLCAD-deficient animals became lethargic and hypotonic during the cold fast challenge (**Supplementary Video S1**). In contrast, rAAV9-treated animals as well as the wild-type animals did not display lethargy and hypotonia as can be appreciated (**Supplementary Videos S2** and **S3**).

Hypoketotic hypoglycemia is a primary presenting symptom for in VLCAD-deficient patients. Blood glucose levels were compared in all three strains, in fed, fasted, and cold challenge state. There were no significant differences between any of the groups at the fed levels, however, blood glucose levels were significantly reduced following both at fasting and cold challenge in the PBS control VLCAD-deficient animals when compared to the wild-type mice (**Figure 6c**). In contrast, the rAAV9-VLCAD-treated animals fully corrected glucose levels to that of wild-type under all conditions. One wild-type mouse had blood glucose levels of 278 mg/dl, which drove the average up in the wild-type after the cold fast challenge. However, blood glucose levels after the cold fast challenge, were not significantly different from the VLCAD$^{-/-}$ rAAV9-treated and the wild-type mice, whereas VLCAD$^{-/-}$ animals blood glucose levels were significantly reduced.

DISCUSSION

Phenotypic correction of multiple disease-specific phenotypes, including blood acyl carnitines, thermoregulation, resistance to lethargy, and blood glucose maintenance was shown here using of

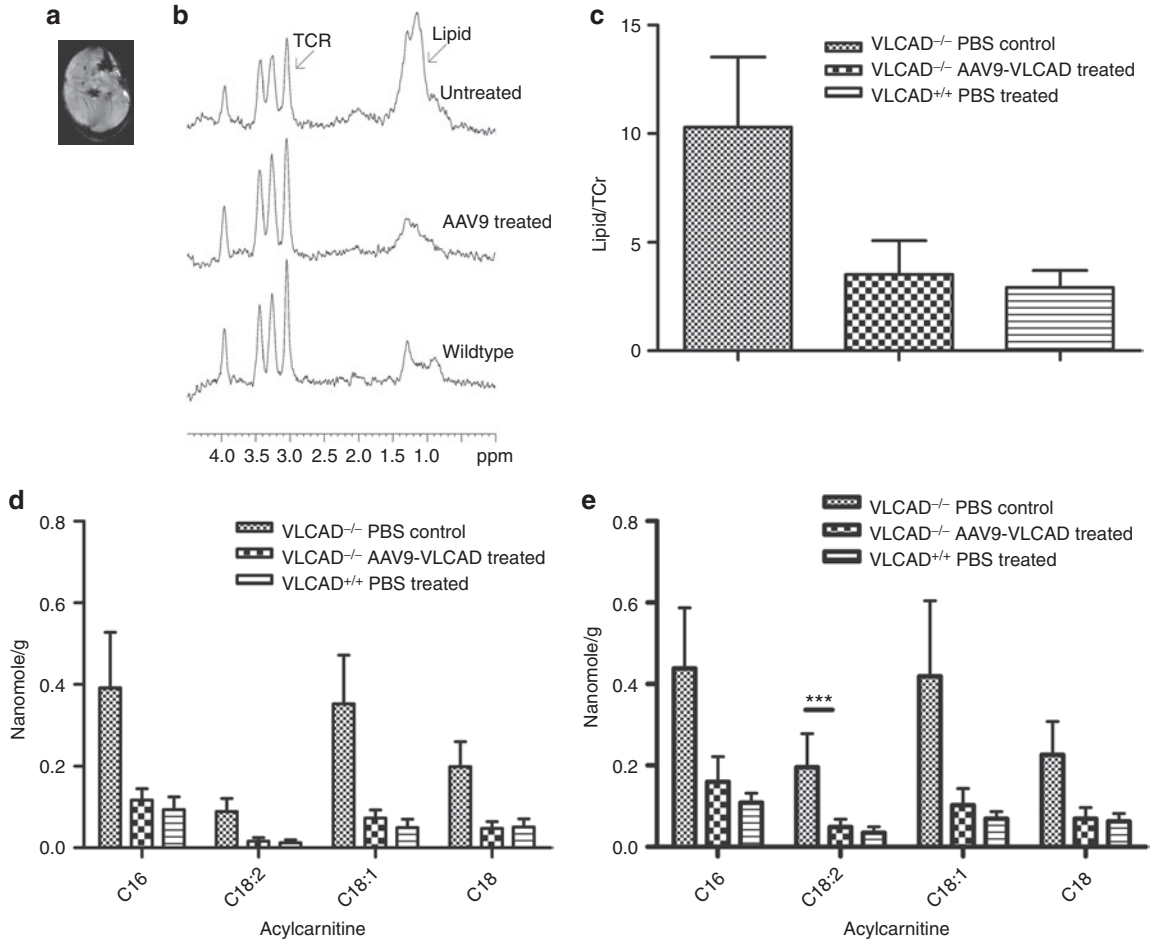

Figure 4 Reduction of lipids in the muscle of corrected mice *in vivo* and *ex vivo*. *$P < 0.05$, **$P < 0.01$, ***$P < 0.001$. (**a**) Magnetic resonance image (MRI) of hindlimb muscle 12–14 weeks postinjection. (**b**) Representative spectra from MRS of muscle *in vivo*. (**c**) Quantification of the ratio of the area of the lipid peak/area of the taurine–creatine peak. $n = 7$ untreated VLCAD$^{-/-}$ controls, $n = 6$ rAAV9-treated VLCAD$^{-/-}$ animals and wild-type controls. Error bars are SEM. (**d**) Mass spectrometry of extensor digitorum longus (EDL) *ex vivo* 21–25 weeks postinjection. $n = 7$ untreated VLCAD$^{-/-}$ controls, $n = 6$ AAV9-treated VLCAD$^{-/-}$ and wild-type controls. Error bars are SEM. Differences were as follows: C16 $P = 0.09$, C18:2 $P = 0.06$ C18:1 $P = 0.06$ C18 $P = 0.05$. Samples were run in triplicate. (**e**) Mass spectrometry of soleus (SOL) *ex vivo* 21–25 weeks postinjection. $n = 7$ untreated VLCAD$^{-/-}$ controls, 6 rAAV9 VLCAD$^{-/-}$ and wild-type controls. Error bars are SEM. Statistics were as follows: C16 NS, C18:2 $P = 0.001$, C18:1 P = NS, C18p = NS.

rAAV9-mediated gene therapy in a mouse model of VLCAD deficiency. Unlike the previous work by Merritt and colleagues,[14] we were able to show long-term expression of VLCAD in all targeted tissues including liver, brown fat, cardiac and skeletal muscle. The difference in long-term expression could have been due to the use of the CBA expression cassette over the CMV promoter, the latter of which is known to be inactivated in the liver in the absence of nuclear factor-kβ.[19] Also the use of rAAV9, which has been shown previously to target tissues involved in fatty acid oxidation after systemic delivery, could have allowed for better systemic correction. A clinically translatable noninvasive technique, MRS, was employed to measure correction within the muscle and liver. Results from the MRS were confirmed with MS/MS of the tissues. Within the liver tissue, accumulates were mildly reduced as detected by MRS and MS/MS but not to the extent seen in other tissues such as skeletal muscle. No previous work concerning correction of disorders of fatty acid oxidation have employed MS/MS of tissue samples to measure accumulations of acyl carnitines within tissues themselves. Correction of short-chain acyl-coA dehydrogenase using rAAV8 showed reduction of liver accumulated by MRS but this was a targeted approach injecting into the portal vein.[10] The VLCAD staining pattern in the liver is different from that within the cardiac and skeletal muscle where it is widespread but at a low level of expression. Within the liver, it appeared that certain cells were expressing VLCAD at very high levels, while other cells were not expressing at all. However without efficient targeting of the liver, reduction of accumulates in the blood as well as maintenance of blood glucose levels would not be expected. This expression pattern may cause the correction discrepancy between whole liver extract accumulations and the impact of the liver on reducing whole blood accumulates and maintaining blood glucose levels. This phenomenon has been previously reported using rAAV8.[20]

Expression of VLCAD in brown fat after systemic injection is also novel. To our knowledge, there have been no reports that have shown transduction of brown adipose tissue and only two reports attempting to target white adipose tissue. Both reports used AAV1 and required an enhancing agent in order to get

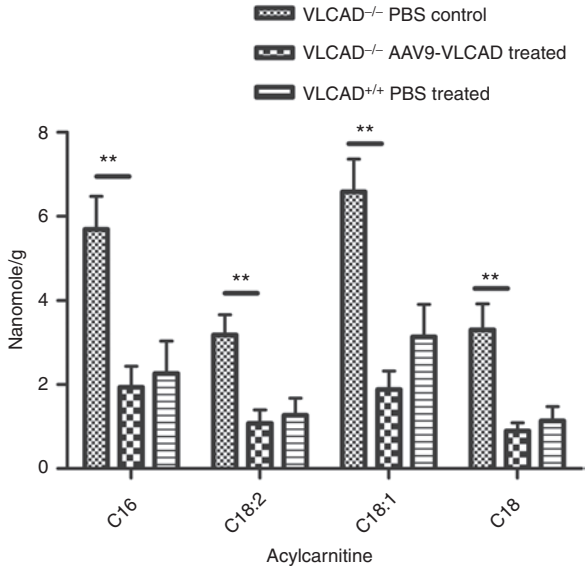

Figure 5 Reduction of acyl carnitines in the heart. *P < 0.05, **P < 0.01, ***P < 0.001, ****P < 0.0001. Mass spectrometry of heart tissue *ex vivo* 21–25 weeks postinjection. n = 7 untreated VLCAD$^{-/-}$ controls, n = 6 AAV9 VCLAD$^{-/-}$ and wild-type controls. Error bars are SEM. Statistics were as follows: C16 P = 0.003 C18:2 P = 0.005 C18:1 P = 0.004 C18 P = 0.005. VLCAD, very long-chain acyl-coA dehydrogenase.

efficient transduction.[21,22] In this report, we were primarily concerned with brown adipose tissue because of its important role in thermogenesis. Brown fat differs from white adipose tissue in that it is highly vascularized, which gives rAAV9 easy access to brown adipose tissue when given systemically however that does not necessarily imply transduction or expression. Transduction was also seen in other tissues including the lung, lymph nodes, spleen and gonads. Detargeting strategies such as capsid mutations and tissue specific promoters and microRNAs may be employed to minimize transduction and expression in unwanted tissues, if this ultimately proves to be necessary.

The pronounced in ability of AAV9-treated VLCAD$^{-/-}$ mice to thermoregulate body temperature in a cold environment compared to the untreated mice clearly demonstrates correction of the cold sensitive phenotype. The role brown fat plays in the phenotypic correction of these mice has yet to be determined; however, it is suspected that brown fat is not solely responsible for temperature maintenance during the cold fast challenge. Brown fat plays an important role in nonshivering thermogenesis by expressing UCP-1 protein, which allows uncoupling of oxidative phosphorylation and the production of heat. Brown fat has a vital role in thermogenesis in newborns, and is present and functional in adult humans although to a lesser extent.[23] Work by Skilling and colleagues,[24] suggests that brown fat does not play as strong of a role in VLCAD-deficient sensitivity to cold as it does in shorter chain deficient animals such as short-chain acyl-coA dehydrogenase. They suggest that rapid consumption of glycogen in the liver and muscle as well as impaired ability to shiver and decreased cardiac function is responsible for cold sensitivity.[24] Unlike other disorders of fatty acid oxidation no energy can be produced by fatty acid oxidation, as VLCAD is the rate-limiting enzyme. Exil and collegues,[25] report that VLCAD-

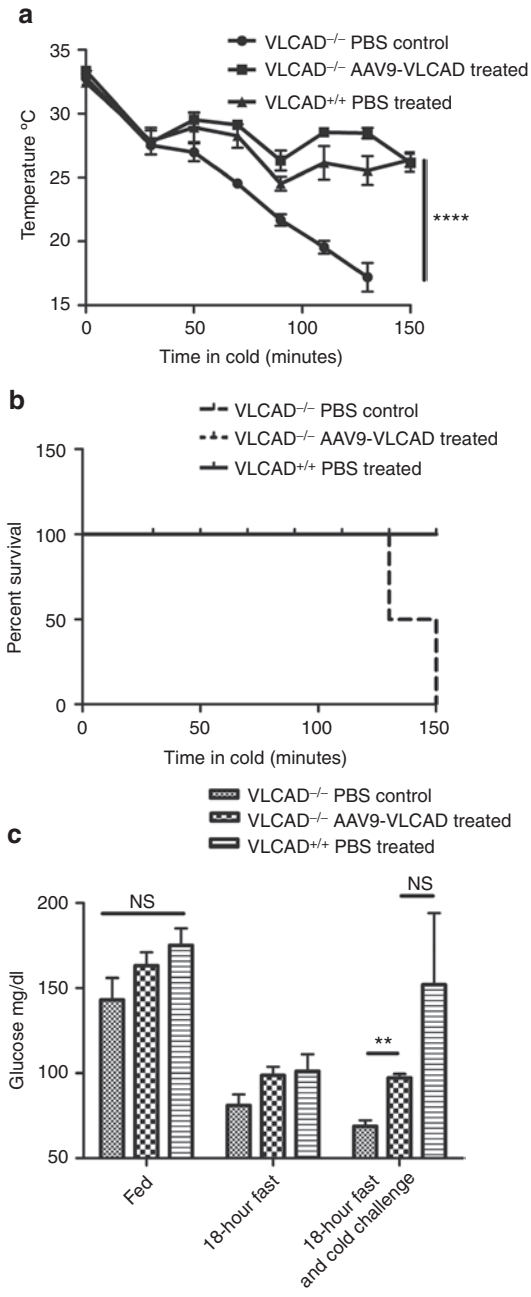

Figure 6 Phenotypic correction with rAAV9-very long-chain acyl-coA dehydrogenase (VLCAD)-treated mice after cold fast challenge. *P < 0.05, **P < 0.01, ***P < 0.001, ****P < 0.0001 and NS = not significant. (**a**) Core body temperature of mice undergoing cold fast challenge, temperatures were recorded every 20 minutes by rectal thermometer. Mice were humanely sacrificed if body temperatures dropped below 20 °C, n = 4. Error bars are SEM. P = value by two-way analysis of variance (ANOVA) $P \leq 0.0001$. (**b**) Survival of cold fast challenge. (**c**) Blood glucose levels during fed, fasted and fasted plus cold challenge conditions, n = 4. Error bars are SEM. No significant difference at fed state between all groups or between rAAV9-treated animals and wild-type under any condition, P = 0.005.

deficient animals succumb to bradycardia, during the cold fast challenge. Therefore, both shivering and nonshivering thermogenesis may play a role in the defect in thermoregulation in these mice. rAAV-mediated expression of VLCAD in liver, allowing the

animal to produce ketones which can go on to produce energy in other tissues may have a larger impact on thermogenesis than expression of VLCAD in the brown fat as VLCAD-deficient mice retain 80% residual activity in the brown fat.[24] Also rAAV-mediated expression of VLCAD in the muscle may allow for heat production through shivering. Correction of multiple tissues may be necessary in order to see correction of this phenotype.

Current standard of care for VLCAD patients is primarily dietary, limiting long-chain fatty acids and supplementing with medium chains as well as avoidance of fasting. Studies have shown effectiveness, especially when administered prior to exercise.[26,27] However, even with screening and treatment, ~10–20% of patients suffer episodic rhabdomyolysis.[28] Supplementation of medium-chain triglycerides has come under question since patients can suffer myopathic symptoms despite treatment and studies in VLCAD-deficient mice have shown muscle phenotypes after exercise on fat-reduced carbohydrate-enriched diets.[29] Also mice fed a diet of medium-chain triglycerides had accumulations of visceral fat and liver lipids as well as tissue fat composition changed significantly.[8] Although patients diagnosed by newborn screening have greatly reduced mortality associated with all disorders of fatty acid oxidation, sudden death has still been reported.[30] Having a therapy rather than treatment options could vastly improve patient's quality of life. This work provides proof-of-concept for rAAV9-mediated gene therapy for VLCAD deficiency.

MATERIALS AND METHODS

Animals. VLCAD$^{-/-}$ mice were created by Exil *et al.* and purchased from Mutant Mouse Regional Resource Centers (MMRC, University of Missouri, Columbia, MO). VLCAD$^{-/-}$ was created by breeding VLCAD$^{-/+}$ animals creating VLCAD$^{-/-}$ and VLCAD$^{+/+}$ littermate controls. Mice were maintained in a pathogen-free facility with 12-hour light and dark schedule. Mice were fed PicoLab Mouse Diet 20 5058 (LabDiet, Richmond IN) until 2 weeks postinjection and then were placed on a standard chow. Mice received both diets and water *ad libitum*. Animals were fasted for 18–24 hours before bleeds, magnetic resonance spectrometry or cold fast challenge. For cold fast challenge, after the 18-hour fast, mice were singly housed in minimal bedding cages and placed in a 4 °C cold room for 150 minutes or until rectal temperatures were below 20 °C. Blood glucose levels were measured by Nova Max Glucose Monitor and Strips (Nova Biomedical, Waltham, MA).

All animal procedures were approved by University of Massachusetts Medical School Institutional Animal Care and Use Committee as well as University of Florida Institutional Animal Care and Use Committee in accordance with the Association for Assessment and Accreditation of Laboratory Animal Care International specifications.

rAAV vectors. rAAV9/2 pseudotyped vectors were generated to express human VLCAD under the transcriptional control of the cytomegalovirus enhancer/chicken β-actin promoter.[19] rAAV vectors were produced, purified and tittered as previously described (UMMS Gene Therapy Center, Worcester, MA).[31]

Genomic DNA extraction and quantitative-PCR. DNA was extracted and quantified as previously described.[32] Animals were sacrificed at indicated time points and tissues were harvested in a manner to avoid cross-contamination, snap frozen in liquid nitrogen and stored at −80 °C. gDNA was extracted using a DNeasy blood and tissue kit (Qiagen, Valencia, CA) according to the manufacturer's instructions. gDNA concentrations were determined using an Eppendorf Biophotometer (Eppendorf, Hamburg, Germany).

rAAV genome copies in the gDNA from heart, liver, tibialis anterior, and brown fat were quantified by quantitative-PCR with an ABI 7900 HT sequence detection system (Applied Biosystems, Carlsbad, CA) according to the manufacturer's instructions and results were analyzed using SDS 2.3 software. Briefly, primers and probe were designed to amplify SV40 poly-A tail of the rAAV9-CBA-VLCAD vector. A standard curve was generated using plasmid DNA containing the same SV40 poly-A target sequence. PCR contained a total volume of 100 µl and were run at the following conditions: 50 °C for 2 minutes, 95 °C for 10 minutes, and 45 cycles of 95 °C for 15 seconds and 60 °C for 1 minute.

DNA samples were assayed in triplicate. In order to assay PCR inhibition, the third replicate was spiked with plasmid DNA at a ratio of 100-copies/µg gDNA. If this replicate was greater than 40-copies/µg gDNA then the results were considered acceptable. If a sample contained greater than or equal to 100-copies/µg gDNA it was considered positive for vector genomes. If a sample contained less than 100 copies/µg gDNA it was considered negative for vector genomes. If less than 1 µg of gDNA was analyzed to avoid PCR inhibition, the vector copy number reported was normalized per µg gDNA and the plasmid spike in was reduced to maintain the ratio of 100-copies/µg gDNA.

Immunohistochemistry. Tissues were fixed in 10% neutral buffered formalin, and embedded in paraffin. Immunohistochemistry was carried out by the Molecular Pathology and Immunology Core at University of Florida using the DAKO Autostainer plus protocol. Briefly, 4 µm serial sections were removed of paraffin and incubated with 3% H_2O_2 in methanol to block endogenous peroxidase activity. Sections were treated with Trilogy (Cell Marque, Rocklin, CA) at 95 °C for 25 minutes and blocked with Sniper (Biocare Medical, Walnut Creek, CA) to reduce nonspecific background staining. Sections were incubated with rabbit anti-mouse VLCAD at room temperature for 1 hour. Then sections were incubated with Mach2 Gt × Rb HRP polymer (Biocare Medical) for 30 minutes. Staining was visualized with DAB chromagen (Biocare Medical).

Mass spectrometry. Blood acyl carnitines were extracted, derivatized, and analyzed as described previously.[33] The following labeled carnitine standards (Cambridge Isotope Laboratories, Andover, MA) were used for quantification: L-Carnitine (*N*-trimethyl-D_9), L-acetylcarnitine (*N*-methyl-D_3), L-propionylcarnitine (*N*-methyl-D_3), L-butyrylcarnitine (*N*-methyl-D_3), L-isovalerylcarnitine (*N*-trimethyl-D_9), L-octanoylcarnitine (*N*-methyl-D_3), L-myristoylcarnitine (*N*-trimethyl-D_9) and L-palmitoylcarnitine (*N*-methyl-D_3). Blood acyl carnitine samples were analyzed as butyl esters on a Micromass Quattro II (Manchester, UK) with an electrospray ionization source operating in the positive ion mode by direct infusion. Tissue samples were processed as previously described.[34] In brief, frozen tissue samples were ground into powder and resuspended in 80% acetonitrile containing carnitine standards described above at a concentration of 60 mg/ml. Samples were homogenized and centrifuged, supernatants were dried under nitrogen. Samples were then resuspended in 10% acetyl chloride in 1-butanol and heated at 65 °C for 15 minutes, dried under nitrogen and brought up in 80% acetonitrile for analysis. Samples were run in triplicate on a Waters (Milford, MA) Premier XE triple quadrupole mass spectrometer similarly to the blood samples.

^{1}H-MRS. Single voxel ^{1}H-MRS was obtained from the tibialis anterior muscle and liver at 11.1T and 4.7T, respectively. 11.1T localized proton muscle spectra were obtained using a Bruker spectrometer (PV3) as described previously.[9] A custom-made loop gap coil with 1.4-cm inner diameter tuned to 470.5 MHz was used. Localizer anatomical proton magnetic resonance images were acquired using FLASH (matrix, 256 × 256; echo time = 4.3 msec; repetition time = 207 msec, FOV = 20 × 20 mm^2) were acquired in three orthogonal directions for the precise localization of a volume of interest from which proton MRS would be obtained. Water suppression was optimized by chemical shift-selective water suppression. Localized spectra were acquired by point-resolved spatially localized spectroscopy (echo time = 18 msec; repetition time = 3,000 msec; number of excitations = 512, bandwidth = 8,013 Hz, number

of complex points = 2,048). Data were processed using jMRUI (http://www.mrui.uab.es/mrui/mrui_Overview.shtml). Similarly localized single voxel proton liver spectra were obtained at 4.7T using point-resolved spatially localized spectroscopy (echo time = 14 msec; repetition time = 2,500 msec; number of excitations = 16, bandwidth = 3,005 Hz, number of complex points = 8,196) on a Varian/Agilent spectrometer. Liver MRS was processed using in house software (IDL; ITT) in order to determine the integral of water and lipid resonances.

Statistics. All statistics were carried out using Prism 5 Software (GraphPad Software, San Diego, CA). All data are presented as means ± SEM. The *n* value designates number of animals used. Significant differences were determined by unpaired Student's *t*-test. When looking at the effect of two variables, such as reduction of acyl carnitines and time, or temperature and time, a two-way analysis of variance were used to determine significance. Differences were considered significant if $P < 0.05$.

SUPPLEMENTARY MATERIAL

Figure S1. Inflammation of liver postinjection.
Figure S2. Reduction of acyl carnitines in rAAV9-VLCAD with GFP control.
Figure S3. Acyl carnitine profiles over time in uninjected mice.
Video S1. Representative video of VLCAD$^{-/-}$ PBS control mouse after 18-hour fast and 120 minutes at 4 °C.
Video S2. Representative video of VLCAD$^{-/-}$ AAV9-treated mouse after 18-hour fast and 150 minutes at 4 °C.
Video S3. Representative video of VLCAD$^{+/+}$ PBS control mouse after 18-hour fast and 150 minutes at 4°C.

ACKNOWLEDGMENTS

We acknowledge the PGTC Toxicology Core, UMass Vector Core, and UMass Mass Spectrometry Core. NMR (MRI) data was supported through the National High Magnetic Field Laboratory and obtained at the Advanced Magnetic Resonance Imaging and Spectroscopy (AMRIS) facility in the McKnight Brain Institute of the University of Florida.

REFERENCES

1. Spiekerkoetter, U, Sun, B, Zytkovicz, T, Wanders, R, Strauss, AW and Wendel, U (2003). MS/MS-based newborn and family screening detects asymptomatic patients with very-long-chain acyl-CoA dehydrogenase deficiency. *J Pediatr* **143**: 335–342.
2. Arnold, GL, Van Hove, J, Freedenberg, D, Strauss, A, Longo, N, Burton, B *et al.* (2009). A Delphi clinical practice protocol for the management of very long chain acyl-CoA dehydrogenase deficiency. *Mol Genet Metab* **96**: 85–90.
3. Vianey-Saban, C, Divry, P, Brivet, M, Nada, M, Zabot, MT, Mathieu, M *et al.* (1998). Mitochondrial very-long-chain acyl-coenzyme A dehydrogenase deficiency: clinical characteristics and diagnostic considerations in 30 patients. *Clin Chim Acta* **269**: 43–62.
4. Smelt, AH, Poorthuis, BJ, Onkenhout, W, Scholte, HR, Andresen, BS, van Duinen, SG *et al.* (1998). Very long chain acyl-coenzyme A dehydrogenase deficiency with adult onset. *Ann Neurol* **43**: 540–544.
5. Gregersen, N, Andresen, BS, Corydon, MJ, Corydon, TJ, Olsen, RK, Bolund, L *et al.* (2001). Mutation analysis in mitochondrial fatty acid oxidation defects: Exemplified by acyl-CoA dehydrogenase deficiencies, with special focus on genotype-phenotype relationship. *Hum Mutat* **18**: 169–189.
6. Online Medelian Inheritance in Man, O.J.H.U., Baltimore, MD. MIM Number: 201475: 27 April 2011.
7. Pons, R, Cavadini, P, Baratta, S, Invernizzi, F, Lamantea, E, Garavaglia, B *et al.* (2000). Clinical and molecular heterogeneity in very-long-chain acyl-coenzyme A dehydrogenase deficiency. *Pediatr Neurol* **22**: 98–105.
8. Tucci, S, Flögel, U, Sturm, M, Borsch, E and Spiekerkoetter, U (2011). Disrupted fat distribution and composition due to medium-chain triglycerides in mice with a ß-oxidation defect. *Am J Clin Nutr* **94**: 439–449.
9. Conlon, TJ, Walter, G, Owen, R, Cossette, T, Erger, K, Gutierrez, G *et al.* (2006). Systemic correction of a fatty acid oxidation defect by intramuscular injection of a recombinant adeno-associated virus vector. *Hum Gene Ther* **17**: 71–80.
10. Beattie, SG, Goetzman, E, Conlon, T, Germain, S, Walter, G, Campbell-Thompson, M *et al.* (2008). Biochemical correction of short-chain acyl-coenzyme A dehydrogenase deficiency after portal vein injection of rAAV8-SCAD. *Hum Gene Ther* **19**: 579–588.
11. Beattie, SG, Goetzman, E, Tang, Q, Conlon, T, Campbell-Thompson, M, Matern, D *et al.* (2008). Recombinant adeno-associated virus-mediated gene delivery of long chain acyl coenzyme A dehydrogenase (LCAD) into LCAD-deficient mice. *J Gene Med* **10**: 1113–1123.
12. Inagaki, K, Fuess, S, Storm, TA, Gibson, GA, Mctiernan, CF, Kay, MA *et al.* (2006). Robust systemic transduction with AAV9 vectors in mice: efficient global cardiac gene transfer superior to that of AAV8. *Mol Ther* **14**: 45–53.
13. Zincarelli, C, Soltys, S, Rengo, G and Rabinowitz, JE (2008). Analysis of AAV serotypes 1-9 mediated gene expression and tropism in mice after systemic injection. *Mol Ther* **16**: 1073–1080.
14. Merritt, JL 2nd, Nguyen, T, Daniels, J, Matern, D and Schowalter, DB (2009). Biochemical correction of very long-chain acyl-CoA dehydrogenase deficiency following adeno-associated virus gene therapy. *Mol Ther* **17**: 425–429.
15. Bonnet, D, Martin, D, Pascale De Lonlay,, Villain, E, Jouvet, P, Rabier, D *et al.* (1999). Arrhythmias and conduction defects as presenting symptoms of fatty acid oxidation disorders in children. *Circulation* **100**: 2248–2253.
16. Mathur, A, Sims, HF, Gopalakrishnan, D, Gibson, B, Rinaldo, P, Vockley, J *et al.* (1999). Molecular heterogeneity in very-long-chain acyl-CoA dehydrogenase deficiency causing pediatric cardiomyopathy and sudden death. *Circulation* **99**: 1337–1343.
17. Laforêt, P, Acquaviva-Bourdain, C, Rigal, O, Brivet, M, Penisson-Besnier, I, Chabrol, B *et al.* (2009). Diagnostic assessment and long-term follow-up of 13 patients with Very Long-Chain Acyl-Coenzyme A dehydrogenase (VLCAD) deficiency. *Neuromuscul Disord* **19**: 324–329.
18. Spiekerkoetter, U, Tokunaga, C, Wendel, U, Mayatepek, E, Exil, V, Duran, M *et al.* (2004). Changes in blood carnitine and acylcarnitine profiles of very long-chain acyl-CoA dehydrogenase-deficient mice subjected to stress. *Eur J Clin Invest* **34**: 191–196.
19. Xu, L, Daly, T, Gao, C, Flotte, TR, Song, S, Byrne, BJ *et al.* (2001). CMV-beta-actin promoter directs higher expression from an adeno-associated viral vector in the liver than the cytomegalovirus or elongation factor 1 alpha promoter and results in therapeutic levels of human factor X in mice. *Hum Gene Ther* **12**: 563–573.
20. Conlon, TJ, Cossette, T, Erger, K, Choi, YK, Clarke, T, Scott-Jorgensen, M *et al.* (2005). Efficient hepatic delivery and expression from a recombinant adeno-associated virus 8 pseudotyped alpha1-antitrypsin vector. *Mol Ther* **12**: 867–875.
21. Mizukami, H, Mimuro, J, Ogura, T, Okada, T, Urabe, M, Kume, A *et al.* (2006). Adipose tissue as a novel target for *in vivo* gene transfer by adeno-associated viral vectors. *Hum Gene Ther* **17**: 921–928.
22. Zhang, FL, Jia, SQ, Zheng, SP and Ding, W (2011). Celastrol enhances AAV1-mediated gene expression in mice adipose tissues. *Gene Ther* **18**: 128–134.
23. Cannon, B and Nedergaard, J (2004). Brown adipose tissue: function and physiological significance. *Physiol Rev* **84**: 277–359.
24. Skilling, H, Coen, PM, Fairfull, L, Ferrell, RE, Goodpaster, BH, Vockley, J *et al.* (2010). Brown adipose tissue function in short-chain acyl-CoA dehydrogenase deficient mice. *Biochem Biophys Res Commun* **400**: 318–322.
25. Exil, VJ, Gardner, CD, Rottman, JN, Sims, H, Bartelds, B, Khuchua, Z *et al.* (2006). Abnormal mitochondrial bioenergetics and heart rate dysfunction in mice lacking very-long-chain acyl-CoA dehydrogenase. *Am J Physiol Heart Circ Physiol* **290**: H1289–H1297.
26. Behrend, AM, Harding, CO, Shoemaker, JD, Matern, D, Sahn, DJ, Elliot, DL *et al.* (2012). Substrate oxidation and cardiac performance during exercise in disorders of long chain fatty acid oxidation. *Mol Genet Metab* **105**: 110–115.
27. Primassin, S, Tucci, S, Herebian, D, Seibt, A, Hoffmann, L, ter Veld, F *et al.* (2010). Pre-exercise medium-chain triglyceride application prevents acylcarnitine accumulation in skeletal muscle from very-long-chain acyl-CoA-dehydrogenase-deficient mice. *J Inherit Metab Dis* **33**: 237–246.
28. Wilcken, B (2010). Fatty acid oxidation disorders: outcome and long-term prognosis. *J Inherit Metab Dis* **33**: 501–506.
29. Primassin, S, Tucci, S and Spiekerkoetter, U (2011). Hepatic and muscular effects of different dietary fat content in VLCAD deficient mice. *Mol Genet Metab* **104**: 546–551.
30. Yusupov, R, Finegold, DN, Naylor, EW, Sahai, I, Waisbren, S and Levy, HL (2010). Sudden death in medium chain acyl-coenzyme a dehydrogenase deficiency (MCADD) despite newborn screening. *Mol Genet Metab* **101**: 33–39.
31. Gao, G, Alvira, MR, Somanathan, S, Lu, Y, Vandenberghe, LH, Rux, JJ *et al.* (2003). Adeno-associated viruses undergo substantial evolution in primates during natural infections. *Proc Natl Acad Sci USA* **100**: 6081–6086.
32. Cideciyan, AV, Aleman, TS, Boye, SL, Schwartz, SB, Kaushal, S, Roman, AJ *et al.* (2008). Human gene therapy for RPE65 isomerase deficiency activates the retinoid cycle of vision but with slow rod kinetics. *Proc Natl Acad Sci USA* **105**: 15112–15117.
33. Zytkovicz, TH, Fitzgerald, EF, Marsden, D, Larson, CA, Shih, VE, Johnson, DM *et al.* (2001). Tandem mass spectrometric analysis for amino, organic, and fatty acid disorders in newborn dried blood spots: a two-year summary from the New England Newborn Screening Program. *Clin Chem* **47**: 1945–1955.
34. Spiekerkoetter, U, Tokunaga, C, Wendel, U, Mayatepek, E, Ijlst, L, Vaz, FM *et al.* (2005). Tissue carnitine homeostasis in very-long-chain acyl-CoA dehydrogenase-deficient mice. *Pediatr Res* **57**: 760–764.